PCP-51

Submitted 2 November 2010

Revised 16 February 2011

Revised 23 March 2011

Local transport characteristics of break junction in Sr_2RuO_4 microbridge

H. Kambara [a,*], S. Kashiwaya [b], H. Kashiwaya [b], Y. Tanaka [c], Y. Maeno [d]

[a] Faculty of Education, Shinshu University, Nagano 380-8544, Japan

[b] National Institute of Advanced Industrial Science and Technology (AIST), Tsukuba 305-8568, Japan

[c] Department of Applied Physics, Nagoya University, Nagoya 464-8603, Japan

[d] Department of Physics, Kyoto University, Kyoto 606-8502, Japan

Abstract

We have measured tunnel conductance of spin-triplet superconductor Sr_2RuO_4 (SRO) break junction which was made by micro fabrication technique with a focused ion beam. This is a new type of tunnel junctions made of SRO, which is different from those made of SRO and other materials. Since the tunnel conductance is sensitive to the internal phase of superconductivity, it enables us to examine the chiral *p*-wave pairing state, which is the most probable candidate of SRO. The tunnel conductance spectrum of the junction showed a broad zero-bias conductance peak whose shape is different from that of high-T_c cuprate superconductors. The shape of the spectrum is in quite good agreement with the calculated spectrum of a chiral *p*-wave/insulator/normal metal junction.

PACS codes: 74.70.Pq, 74.45.+c, 74.78.Na

Keywords: Ruthenates; Chiral *p*-wave; Proximity effect; Tunneling phenomena, Break junction

* Corresponding author.

Dr. Hiroshi Kambara

Postal address: Faculty of Education, Shinshu University, 6-ro, Nishinagano, Nagano 380-8544, Japan

Phone: +81-26-238-4123

Fax: +81-26-234-5540

E-mail address: kambara@shinshu-u.ac.jp

1. Introduction

A strontium ruthenate compound Sr_2RuO_4 (SRO) is now believed to be the spin-triplet *p*-wave pairing superconductor with the superconducting transition temperature (T_c) of 1.5 K. The superconducting order parameter is represented by the so-called chiral *p*-wave state, such as p_x+ip_y [1]. Since this is rewritten to the form of $\exp(i\phi)$, where ϕ is a momentum-dependent phase of the pair potential, the internal phase of the pairing state in SRO is continuously changed from 0 to 2π. This is different from the other anisotropic superconductors, for example, *d*-wave state of high-T_c cuprates in which only two values of 0 or π (the plus or minus sign) are valid. Tunnel spectroscopy along a conducting plane is one of the most powerful methods to investigate anisotropy of the superconducting pairing state [2,3]. Thus it is quite important to carry out tunnel junction experiment for SRO in order to verify the chiral *p*-wave state. So far, several *in-plane* tunnel junction experiments for SRO/other materials have been performed, such as SRO/Pt point contact [4], and 3-Kelvin (3-K) phase/Ru [5,6] junctions. Here the 3-K phase is the interface superconductivity between SRO and Ru inclusion in SRO-Ru eutectic system [7,8]. In this paper, we show a new type of tunnel junction experiment using SRO break junction. The break junction was formed in a microbridge region which was made by micro fabrication technique with a focused ion beam (FIB) [9,10]. We observed a widely distributed zero-bias conductance peak (ZBCP), which is in contrast to a sharp ZBCP observed in high-T_c cuprate/insulator/normal metal junctions [2,11]. We found that the shape of the conductance peak agrees with theoretical calculation of chiral *p*-wave/insulator/normal metal junction, which supports realization of the chiral *p*-wave state in SRO.

2. Experimental

In this experiment, we used an SRO-Ru eutectic crystal grown in an infrared image furnace by the floating zone method [12]. The details of sample preparation before FIB process are shown elsewhere [13]. The sample neck between voltage-lead contacts was milled by FIB to make a microbridge where electrical resistance is dominated. To make *c*-axis path, two alternate parallel slits along *c*-axis were milled [10]. The microbridge region (2 μm × 2.3 μm wide in *ab*-plane, and 1 μm length along *c*-axis as seen in Fig. 1(a) and 1(b)) was selected in Ru-inclusion free region by checking a scanning ion microscope (SIM) image. Some electrical shock or thermal shock induces a crack and forms a break junction (a dark rectangular region in Fig. 1(a)) in the weak microbridge region. However, the formation condition of the break junction is not fully controllable at present. The tunnel conductance measurement was performed using a standard lock-in technique by AC modulation with an amplitude of 2 μA_{rms}. The sample was cooled down to 0.5 K using a ^{3}He cryostat, in which the sample was immersed in liquid ^{3}He directly.

3. Results and Discussion

The differential resistance at zero-bias current (R)-temperature (T) curve of this sample is shown in Fig. 2. We note that the R is slightly decreased even below 1.5 K, the bulk T_c, as seen in the inset of Fig. 2. This means that the tunnel conductance at zero-bias current is increased below T_c.

Figure 3 shows the differential conductance-voltage (dI/dV-V) spectra normalized at 2.8 K. The widely distributed ZBCPs were clearly observed. The peak heights are getting increased with lowering temperature reflecting the decrease of R. The important features of the shape of the dI/dV spectrum are not only a broad peak but also rather sharp dips at the edges of the peak (±0.96 mV at 0.60 K). These features were different from those of the high-T_c cuprate (d-wave)/insulator/normal metal junction where the ZBCP is sharp and the dip is broad [2,11]. In this experiment, the ZBCP was observed from higher temperature (~1.7 K) than T_c, which may reflect some existence of the 3-K phase superconductivity although Ru inclusion is not observed in the microbridge region with the SIM image. Here we focus only on the data of the 1.5-K phase (pure SRO) at lower temperatures than T_c.

To analyze the ZBCP in Fig. 4, we fitted calculated spectra to the experimental data for the following two cases: (i) chiral p-wave/insulator/normal metal ($S/I/N$) junction [14,15] and (ii) chiral p-wave/insulator/chiral p-wave ($S/I/S$) junction, since a spectrum calculation of s, d, p_x (*non*-chiral)-wave/insulator/normal metal junction does not show a broad ZBCP with a sharp dip [2,16,17]. Here we considered the simple chiral p-wave form of $d \propto (p_x+ip_y)$ with an isotropic gap for the d-vector order parameter [1]. In the calculation, we assumed a high tunnel barrier condition $Z = 5$, where $Z = mH/\hbar^2 k_F$ is an effective barrier parameter, H is the barrier potential with delta-function form at the interface, m is the effective mass of quasiparticle, k_F is the Fermi wave number, and $\hbar$ is the Planck's constant divided by 2π. We took into account temperature smearing effect due to Fermi distribution function at finite temperature. The calculated peak heights at zero-bias are adjusted to the experimental values by multiplying some numerical factors. As seen in Fig. 4, the calculated spectra of $S/I/N$ configuration are in quite good agreement with the experimental curves. The dip energy is corresponding to the superconducting gap energy (Δ).

On the other hand, calculated spectra in $S/I/S$ configuration are not good agreement with the experimental results. Here we calculated *S*/*I*/*S* spectra using the following approximation. Since the tunnel current from superconductor 1 to superconductor 2 is proportional to $\int_{-\infty}^{\infty} \rho_1 \rho_2 [f(E) - f(E + eV)] dE$, where $\rho_{1(2)}$ is the quasiparticle density of states of the superconductor 1(2), $f(E)$ is the Fermi distribution function, and V is the applied voltage [18], we assumed that $\rho_{1(2)}$ of the superconductor of *S*/*I*/*S* configuration corresponds to the conductance under the high barrier condition ($Z = 5$) in *S*/*I*/*N* junction. This approximation is reasonable because the tunnel conductance under high barrier limit is indistinguishable from the density of states in *s*-wave case [16] and even in the anisotropic superconductor $d_{x^2-y^2}$ case (see Fig. 2(a) in Ref.[2]). However, calculated *S*/*I*/*S* spectrum shows a small peak at the energy of about 2Δ as well as a zero-bias peak (Fig. 4). Thus, *S*/*I*/*S* calculation is difficult to fit to the experimental data.

One of the possible explanations that *S*/*I*/*N* configuration is fitted better than *S*/*I*/*S* is that the break junction acts as a normal metal sandwiched between two insulators in this experiment and forms *S*/*I*/*N*/*I*/*S* configuration. If the resistance of one side of *S*/*I*/*N* junction is dominant compared to the other side of *N*/*I*/*S* one, the measured conductance reflects the *S*/*I*/*N* conductance. Therefore, it is probable that the shape of the tunnel spectrum is well reproduced by *S*/*I*/*N* configuration. The obtained gap magnitude (Δ = 1.0 meV) is comparable with that obtained by the point-contact experiment [4]. However, this value is 2-3 times larger than those obtained by scanning tunneling microscopy/spectroscopy (STM/S) experiments, which show Δ = 0.28-0.50 meV [19-21]. This discrepancy of the gap magnitude is not cleared at present.

We note that we assumed the *ab*-plane (in-plane) tunneling in the above calculations due to the following reason. If the out-of-plane tunneling is dominant, the tunnel spectra should show the gap structures as seen in STM/S experiments [19-21], which is contrary to the experimental result. Thus we assumed in-plane tunneling, though it is difficult to check where the crack exactly lies with an atomic scale. To control and evaluate the break junction configuration quantitatively is a future problem.

4. Summary

We have measured tunnel spectra of Sr_2RuO_4 break junction formed in a microbridge region made by a focused ion beam. The tunnel spectra show broad zero-bias conductance peaks, which are in good agreement with the calculated spectra of the chiral *p*-wave/insulator/normal metal junction. This result supports that the superconducting symmetry of Sr_2RuO_4 is the chiral *p*-wave state.

Acknowledgments

This work was financially supported by a Grant-in-Aid for Scientific Research on Innovative Areas (No.22103002) from MEXT, Grants-in-Aid for Scientific Research (B) (No.22340096) and for Young Scientists (B) (No.21740276) from JSPS, Japan.

References

[1] A. P. Mackenzie, Y. Maeno, Rev. Mod. Phys. 75 (2003) 657.

[2] Y. Tanaka, S. Kashiwaya, Phys. Rev. Lett. 74 (1995) 3451.

[3] S. Kashiwaya, Y. Tanaka, Rep. Prog. Phys. 63 (2000) 1641.

[4] F. Laube, G. Goll, H. v. Löhneysen, M. Fogelström, F. Lichtenberg, Phys. Rev. Lett. 84 (2000) 1595.

[5] Z. Q. Mao, K. D. Nelson, R. Jin, Y. Liu, Y. Maeno, Phys. Rev. Lett. 87 (2001) 037003.

[6] M. Kawamura, H. Yaguchi, N. Kikugawa, Y. Maeno, H. Takayanagi, J. Phys. Soc. Jpn. 74 (2005) 531.

[7] Y. Maeno, T. Ando, Y. Mori, E. Ohmichi, S. Ikeda, S. Nishizaki, S. Nakatsuji, Phys. Rev. Lett. 81 (1998) 3765.

[8] H. Yaguchi, M. Wada, T. Akima, Y. Maeno, T. Ishiguro, Phys. Rev. B 67 (2003) 214519.

[9] H. Kambara, S. Kashiwaya, H. Yaguchi, Y. Asano, Y. Tanaka, Y. Maeno, Phys. Rev. Lett. 101 (2008) 267003.

[10] H. Kambara, T. Matsumoto, H. Kashiwaya, S. Kashiwaya, H. Yaguchi, Y. Asano, Y. Tanaka, Y. Maeno, J. Phys. Soc. Jpn. 79 (2010) 074708.

[11] I. Iguchi, W. Wang, M. Yamazaki, Y. Tanaka, S. Kashiwaya, Phys. Rev. B 62 (2000) R6131.

[12] Z. Q. Mao, Y. Maeno, H. Fukazawa, Mat. Res. Bull. 35 (2000) 1813.

[13] H. Kambara, S. Kashiwaya, H. Yaguchi, Y. Asano, Y. Tanaka, Y. Maeno, Physica C 469 (2009) 1030.

[14] M. Yamashiro, Y. Tanaka, S. Kashiwaya, Phys. Rev. B 56 (1997) 7847.

[15] M. Yamashiro, Y. Tanaka, Y. Tanuma, S. Kashiwaya, J. Phys. Soc. Jpn. 67 (1998) 3224.

[16] G. E. Blonder, M. Tinkham, T. M. Klapwijk, Phys. Rev. B 25 (1982) 4515.

[17] Y. Tanaka, S. Kashiwaya, Phys. Rev. B 70 (2004) 012507.

[18] M. Tinkham, Introduction to Superconductivity, 2nd ed., McGraw-Hill, New York, 1996, Sec. 3.8.

[19] M. D. Upward, L. P. Kouwenhoven, A. F. Morpurgo, N. Kikugawa, Z. Q. Mao, Y.

Maeno, Phys. Rev. B 65 (2002) 220512(R).

[20] C. Lupien, B. I. Barker, S. Dutta, Y. Maeno, J. C. Davis, arXiv:cond-mat/0503317.

[21] H. Suderow, V. Crespo, I. Guillamon, S. Vieira, F. Servant, P. Lejay, J. P. Brison, J. Flouquet, New J. Phys. 11 (2009) 093004.

Figure captions

FIG. 1: (a) Scanning ion microscope image of the microbridge of Sr_2RuO_4 after FIB milling process. The dark region located in the center of the microbridge shows the break junction. (b) Schematic image of the microbridge of (a). The arrows denote the current path directions.

FIG. 2: The differential resistance at zero-bias current (*R*) - temperature (*T*) curve of the microbridge sample. Inset: Magnified *R*-*T* curve below 3 K. The *R* gradually decreases even below T_c.

FIG. 3: The differential conductance (*dI/dV*) normalized at 2.8 K vs voltage (*V*) spectra. Zero-bias conductance peaks are clearly observed below 1.7 K.

FIG. 4: The normalized *dI/dV* vs *V* spectra at T = 0.60 K (a) and 1.3 K (b). The open symbols denote the experimental data. The thick solid lines denote calculated *S*/*I*/*N* conductance spectra of the chiral *p*-wave superconductor. The dashed lines denote calculated *S*/*I*/*S* spectra. The barrier parameter Z = 5 is used for both *S*/*I*/*N* and *S*/*I*/*S* cases.

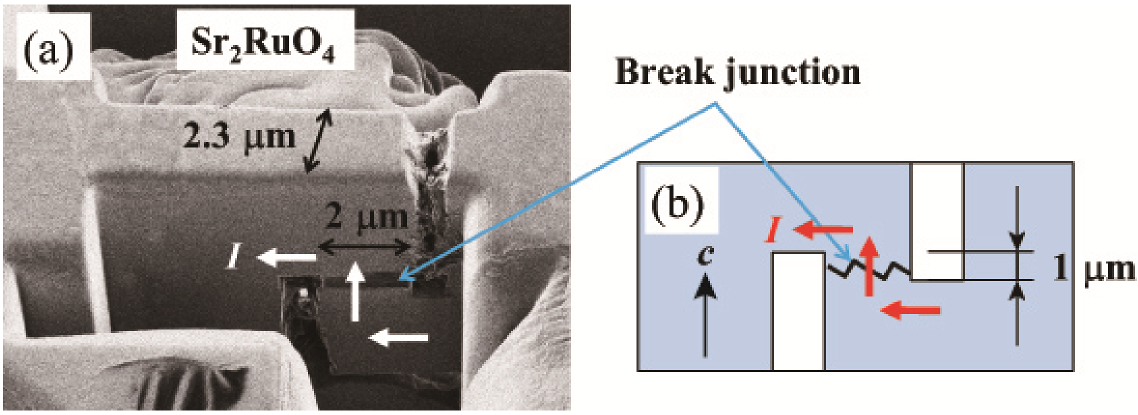

FIG. 1

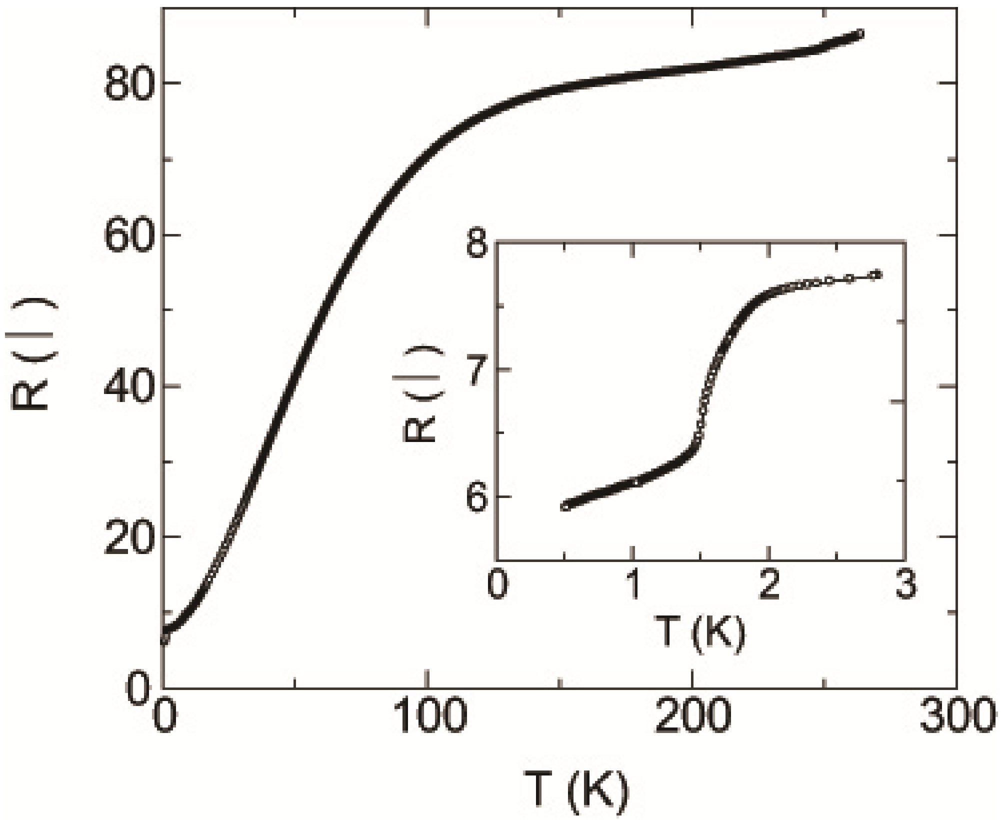

FIG. 2

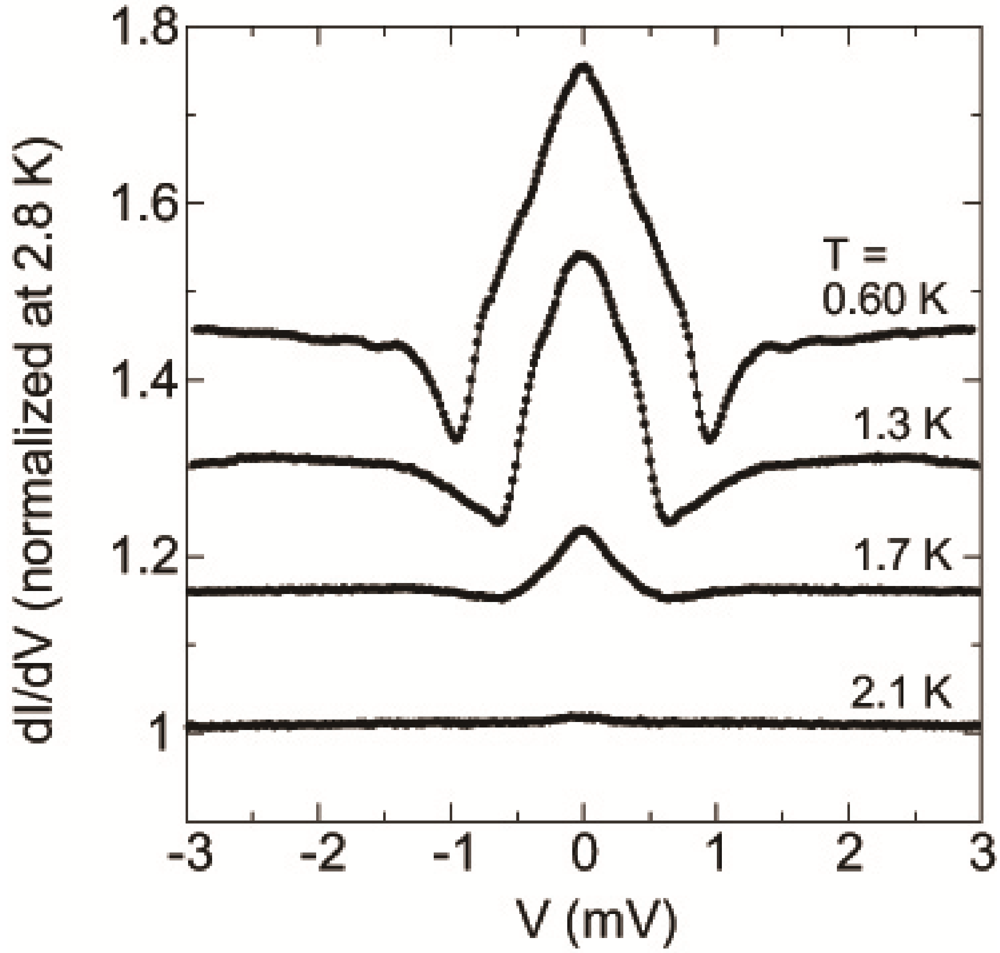

1.8
1.6
1.4
1.2
1
dI/dV (normalized at 2.8 K)
T =
0.60 K
1.3 K
1.7 K
2.1 K
-3
-2
-1
0
1
2
3
V (mV)

FIG. 3

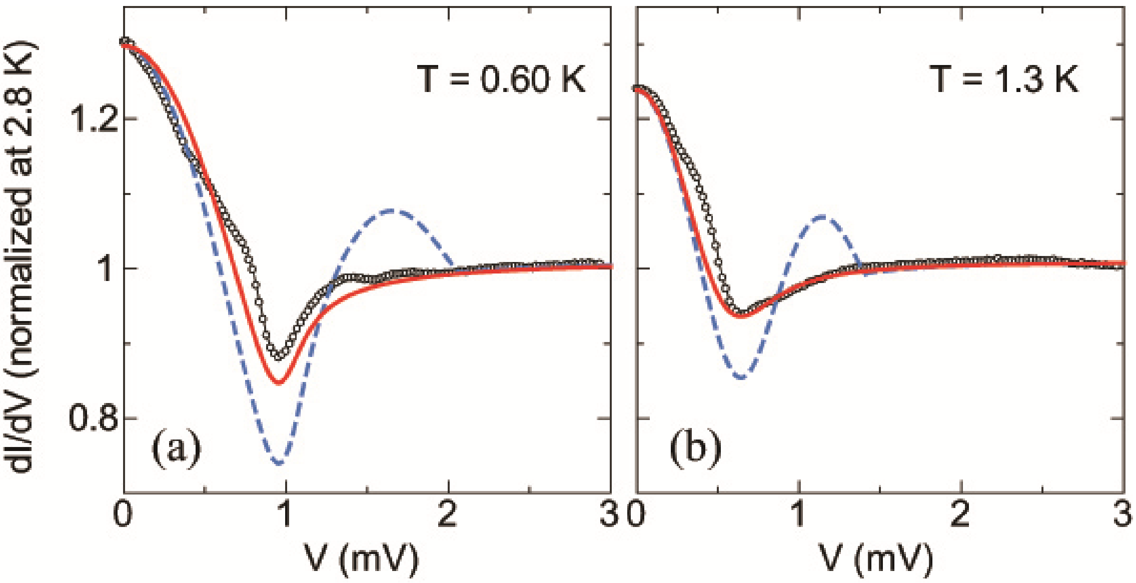

FIG. 4